231941

UCRL-JC-127900
PREPRINT

Optimized Filtering of Regional and Teleseismic Seismograms: Results of Maximizing SNR Measurements From the Wavelet Transform and Filter Banks

Richard R. Leach Jr.
Craig Schultz
Farid Dowla
Lawrence Livermore National Laboratory

This paper was prepared for submittal to the
19th Seismic Research Symposium on Monitoring a CTBT
Orlando, Florida
23-25 September 1997

July 15, 1997

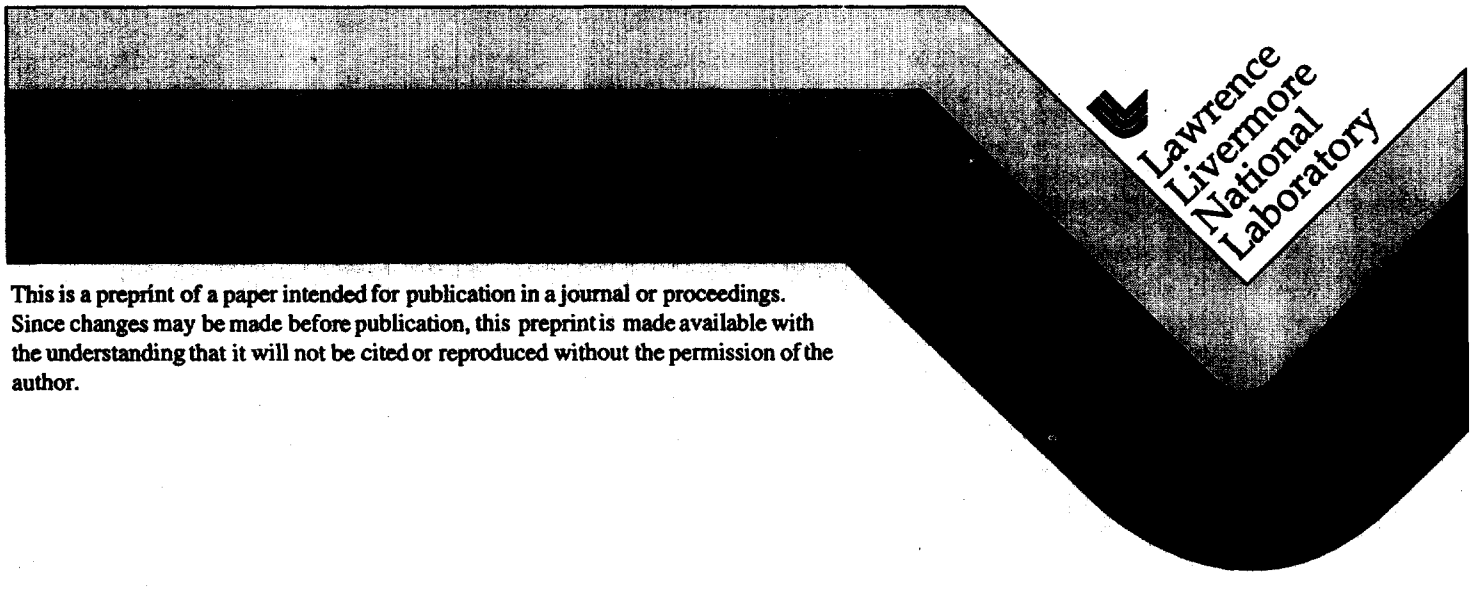

Optimized Filtering of Regional and Teleseismic seismograms: *Results of Maximizing SNR Measurements From the Wavelet Transform and Filter Banks*

Richard R. Leach Jr., Craig Schultz, Farid Dowla

Earth Sciences Division, Lawrence Livermore National Laboratory

Sponsored by DOE CTBT R&D Program[1]

Abstract

Development of a worldwide network to monitor seismic activity requires deployment of seismic sensors in areas which have not been well studied or may have few available recordings. Development and testing of detection and discrimination algorithms requires a robust representative set of calibrated seismic events for a given region. Utilizing events with poor signal-to-noise (SNR) can add significant numbers to usable data sets, but these events must first be adequately filtered. Source and path effects can make this a difficult task, as filtering demands are highly varied as a function of distance, event magnitude, bearing, depth, etc. For a given region, conventional methods of filter selection can be quite subjective and may require intensive analysis of many events. In addition, filter parameters are often overly generalized or contain complicated switching. We have developed a method to provide an optimized filter for any regional or teleseismically recorded event. Recorded seismic signals contain arrival energy which is localized in frequency and time. Localized temporal signals whose frequency content is different from the frequency content of the pre-arrival record are identified using rms power measurements. The method is based on the decomposition of a time series into a set of time series signals or scales. Each scale represents a time-frequency band with a constant Q. SNR is calculated for a pre-event noise window and for a window estimated to contain the arrival. Scales with high SNR are used to indicate the band pass limits for the optimized filter.The results offer a significant improvement in SNR, particularly for low SNR events. Our method provides a straightforward, optimized filter which can be immediately applied to unknown regions as knowledge of the geophysical characteristics is not required. The filtered signals can be used to map the seismic frequency response of a region and may provide improvements in travel-time picking, bearing estimation, regional characterization, and event detection. Results are shown for a set of low SNR events as well as 92 regional and teleseismic events in the Middle East.

Key Words: constant Q filter banks, wavelet transform, calibrated seismic events, Middle East, scales, signal-to-noise

---

1. Research performed under the auspices of the U.S. Department of Energy by the Lawrence Livermore National Laboratory under contract W-7405-ENG-48.

1. OBJECTIVES

The long-term objective of Lawrence Livermore National Laboratory's regionalization research is to provide the U.S. National Data Center (NDC) and the CTBT International Data Center (IDC) with the necessary calibrations and algorithms to improve detection, phase identification, location, and discrimination in the Middle East and North Africa (Dowla, et. al, 1996). To achieve these goals, filtering will play a major role, particularly in low SNR signals. This study uses pre and post-arrival SNR measurements to suggest a filter which will optimize detection and identification of an arrival. This method can be used for any phase arrival, although this study focused on the initial P arrival.

One of the principal challenges was to choose an efficient, but accurate way to decompose the original seismic signal into sub-signals or scales, each of which would emphasize a different frequency band for transient analysis. For this reason, we investigated the application of the wavelet transform as well as simple banks of constant Q filters in order to learn the advantages and drawbacks of each approach.

Our purpose was to measure the SNR with respect to the estimated P arrival in each band and develop and algorithm to identify a subset of bands which together would indicate a filter to produce maximum SNR. This approach has be successfully used to lift observed seismic signals off the background noise with little distortion (Douglas, 1997).

The algorithm was tested in two ways. First, on a small set of low SNR events which were selected by the human analyst based on their difficulty in phase picking. Second, on a set of 92 regional and teleseismic signals recorded at the station ABKT in Alibek, Turkmenistan.

2. RESEARCH ACCOMPLISHED

2.1 Wavelet transforms and constant Q filter banks We considered two approaches to achieve constant Q filtering: the wavelet transform and a constant Q logarithmic filter bank. A discussion on the rapidly growing study of wavelet theory is beyond the scope of this work, but interested readers should refer to a paper by Olivier Rioul (Rioul, et al. 1991) which contains a review, tutorial, and extensive bibliography on wavelet theory. In general, however, the wavelet transform $W(a,\tau)$ of a seismogram signal, $s(\tau)$ is given by:

$$W(a,\tau) = \frac{1}{\sqrt{a}}\int_{-\infty}^{\infty} s(t)h([(t-\tau)]/a)dt \qquad (2.1.1)$$

where a represents the scale and τ time in the transform domain, and $h(t)$ is the analysis wavelet which is localized in both time and frequency (Veterrli, 1995).

One of the key ideas is the decomposition of the original signal into constant relative bandwidth or constant Q frequency bands (Rioul et al., 1991). This approach offers analysis of the data at different scales such that short windows are used at high frequencies and long windows are used at low frequencies. Seismic arrivals often occur in only one or two of the scales.

Of course, constant Q logarithmic filter banks using conventional filters can also be used to decompose seismic signals. Although comparable results are obtained, it is a less efficient approach as it represents each band of a N-point signal with another N-point signal. The discrete wavelet transform represents all scales with a single N-point set. The disadvantage of using wavelets is determining which wavelet basis function to select, and the dyadic nature of the wavelet algorithm, which limits the flexibility in selecting Q values for a given type of data. The results in this report were obtained using constant Q logarithmic filter banks. Figure 2.1.1 illustrates a signal which has been decomposed into scales or filter bands by both the wavelet transform and a 4th order Butterworth constant Q filter bank.

All data used in this study was obtained from the Incorporated Research Institutions in Seismology Data Management Canter (IRIS DMC). Event location, magnitudes, and depths were obtained from the United States Geological Survey Preliminary Determination of Epicenters (USGS/PDE) catalogs. All events used are presumed earthquake signals. All events were recorded using broadband instruments. All stations were 3 element, single site installations. Only the vertical (z) component data was used in this study. RANI and AFIF had a sample rate of 40 Hz. All other stations sampled data at 20 Hz.

Five regional events were chosen by a human analyst to test the algorithm based on their low SNR and analyst difficulty in selecting a filter for picking the P arrival. These five events ranged from 848 to 2332 km. Magnitudes ranged from 3.6 to 4.6 mb. Depths varied from 0 to 79 m. Five different events were recorded at a separate stations as shown in figure 2.1.2. In addition, 92 events recorded at station ABKT in Alibek, Turkmenistan were obtained to examine regional filter clustering. Distances for the ABKT events ranged from 155.2 to 4416.6 km. Magnitudes ranged from 4.3 to 6.2 mb. Event depths varied from 9 to 273 m. A map of these events is also shown in figure 2.1.2.

2.2 Signal and Noise Windows for P arrival Signal and noise windows were selected for each event. The goal was to obtain a noise window which characterized pre-arrival background noise and a signal window which included the P arrival and a small time period surrounding the P arrival. The IASPEI91 model was used to calculate estimated P arrivals for each event. For regional and teleseismic events (>500 km), the signal window was defined from the estimated P arrival -10s to +30s. For local events (< 500 km) the signal window was +-30s centered on the estimated P arrival. The noise window was defined from the 20km/s arrival time to 9/10 of the start time of the signal window. In Figure 2.1.1, the signal and noise windows are the darkened portions of the time series plots.

The instantaneous normalized power $p(t)$ associated with a time-varying signal $x(t)$ is:

$$p(t) = x^2(t) \tag{2.2.1}$$

The average normalized power P is then obtained by a time average of $p(t)$ over a period T.

$$P = \frac{1}{T}\int_0^T x^2(t)dt \tag{2.2.2}$$

The root-mean-square (rms) value X_{rms} is defined as the constant value that produces the same average power as the given time-varying signal. which leads to

$$X_{rms} = \sqrt{P} = \sqrt{\frac{1}{T}\int_0^T x^2(t)dt} \tag{2.2.3}$$

and is denoted by S_{rms} for signal rms power and N_{rms} for noise rms power. Using equation 2.2.3, SNR for this and all other examples is:

$$\text{SNR} = \frac{S_{rms}}{N_{rms}} \tag{2.2.4}$$

2.3 Algorithm for weighing scales or filter bands The 92 ABKT signals were bandpass filtered six times using constant Q 4th order Butterworth filters. The start and stop bands are listed in Figure 2.1.1. The Q used was 1.25 with the lowest bandpass centered around 0.12 to 0.28 Hz. All bands were considered for teleseismic data, the two lowest frequency bands were ignored for regional events, and only the three highest bands were considered for local events.

The SNR value for each band was compared to the SNR value of the original signal. All SNR

values greater than or equal to the original signal's SNR value were classified as potentially useful or 'high SNR' bands. The bands whose SNR value fell below the original signal's SNR value were classified as 'low SNR' bands. The first step was to select the highest frequency 'high SNR' band. If the next lower frequency adjacent band was also a 'high SNR' band, it was concatenated with the previous band. This process continued until a 'low SNR' band was encountered. If none of the bands were 'high SNR' bands, the dominant band was selected as the 'suggested' bandpass filter with the caveat that the signal should be reviewed by a human expert for further analysis.

The result of the above process is a 'suggested' bandpass filter whose band limits a were selected to improve SNR. This filter is then applied to the original signal as the optimal filter for this event. Frequency bands which contain maximum SNR for the desired seismic phase arrival were measured and identified using equation 2.2.4.

This algorithm can be applied using constant Q filter banks, or using the wavelet transform. Analogous to the previous discussion, scales are classified into 'high SNR' and 'low SNR' wavelet scales. The rest of the algorithm is the same. IA conventional filter is used based on the 'suggested' bandlimits represented by the 'high SNR' scales. This is extremely useful, as it avoids the problems associated with anticausal distortion introduced by modifying wavelet scales prior to reconstruction or synthesis.

2.4 Results for low SNR events The events at the top of figure 2.1.1 were described by the human analyst as being difficult or impossible to pick the P arrival from the raw signal without a great amount of uncertainty. Often, the analyst had to 'hunt' for a filter which would bring out the P arrival. The analyst's final selected filter specifications are listed in Figure 2.4.1.

These events were also processed using the algorithm described previously. The filter suggested for optimized SNR was then applied to the original signal. The automatically selected filter specifications are also listed in Figure 2.4.1.

Figure 2.4.1 contains three plots for each event. The top trace is the original raw waveform. The middle trace is the result of applying the analyst selected filter. The bottom trace is the result of applying the automatically selected filter. The vertical line labeled IP is the IASPEI91 P arrival time. (Kennett et al., 1991) The vertical line labeled FP is the P arrival time picked by the analyst. The analyst used the middle trace for the FP pick, although it is also superimposed on the raw and automatic filter trace for comparison.

2.5 Results for 92 ABKT events The filtering algorithm was applied to 92 events recorded at station ABKT. This produced a set of 'suggested' filters which could be readily clustered. Clustering revealed eight unique bandpass filters for the 92 ABKT events. A histogram, plot, and table of filter bandwidths is shown in figure 2.5.1.

From the histogram we see that the predominant filter is the third cluster, corresponding to a suggested frequency bandwidth of 0.55 to 1.52 Hz. This band, which was suggested in over half the events, is interesting in two ways. If the algorithm does indeed produce optimal filtering, then one might argue that the third cluster indicates the best general band for the region. Inspection of the other bands, however, reveals quite a wide variance which would make this approach impractical. Secondly, most of the events fall into the third and fifth cluster. These clusters represent tight bands around a specific center frequency. This suggests that an approach using fixed filter bandpass limits would do poorly in an automated system. For optimal filtering, many events require narrow bandwidths around a specific frequency. Finally, maps with filter cluster symbol size scaled by the reported magnitude and depth are plotted in figure 2.5.2.

2.6 Regional frequency response Figure 2.6.1 is a map of the region surrounding ABKT with a contour map and a surface plot superimposed. The upper map shows the Pn velocity relative to 7.9 km/s. (Hearn et al., 1994) The lower map uses the bandwidth clusters produced by the 92 ABKT events were used to generate the topography. The contours are approximately equal to the center frequency of the cluster bandwidths. From this result, it is clear that stations such as ABKT show complex and highly variable P wave propagation.

CONCLUSIONS AND RECOMMENDATIONS

The extreme geophysical variability of regions in the Middle East as seen at ABKT illustrates the need for methods which can use existing data to produce useful information about the region. We recommend further testing of this approach at other sites in the Middle East and North Africa. It is also recommended that this method be used as a pre-processing step to lower the variance in detection and location algorithms. We recommend that the algorithm be applied to other seismic phases such as surface waves. Further study is needed to determine optimal wavelet basis functions as suggested by others (Gribb et al, 1997, Kawaldip et al. 1997, and Yomogida, 1994) and to modify the wavelet transform itself to allow a selectable Q. A study to determine the optimal Q for seismograms in general would also be very useful. Finally, the implication for CTBT monitoring is that this algorithm offers a simple, effective process which can, in general, produce filtered seismic signals with maximum SNR and bring out signals typically buried in background noise.

REFERENCES

Douglas, A (1997) Bandpass filtering to reduce noise on seismograms: Is there a better way?. *Bull. Seis Soc Am.*, Vol 87, No. 4. pp. 770-777.

Dowla, F. U., P. Goldstein, P. Harben, D. Harris, T. Hauk, S. Jarpe, E. Kansa, P. Lewis, D. McNamara, H. Patton, D. Rock, A. Ryall, C. Schultz, A. Smith, J. Sweeney, W. Walter, L. Wethern (1996) Seismic Regionalization in the Middle East and North Africa, Proceedings of the 18th annual research symposium on monitoring a comprehensive test ban treaty, July, 55-64.

Grub, H. J. and A. T. Walden (1997) Characterizing seismic time series using the discrete wavelet transform. *Geophysical Prospecting*, **45**, 183-205.

Hearn, T. and J. Ni (1994) Pn velocities beneath continental collision zones: the Turkish-Iranian Plateau, Geophys. J. Intl, **117**, 273-283

Kanwaldip, S. A., and F. U. Dowla (1997) Wavelet Transform Methods for Phase Identification in Three-component Seismograms. (in preparation).

Kennett, B. and E. Engdahl (1991) for global earthquake and phase identification. *GJInt.*, **105**, 429-465

Rioul, O. and M. Vetterli (1991) Wavelets and signal processing, *IEEE Spectrum magazine*, October, 14-36.

Vetterli, M., and J. Kovacevic (1995). *Wavelets and Subband Coding*, Prentice Hall, Englewood Cliffs, NJ.

Yomogida, K., (1994) Detection of anomalous seismic phases by the wavelet transform., *Geophys. J. Int.***116**, 119-130.

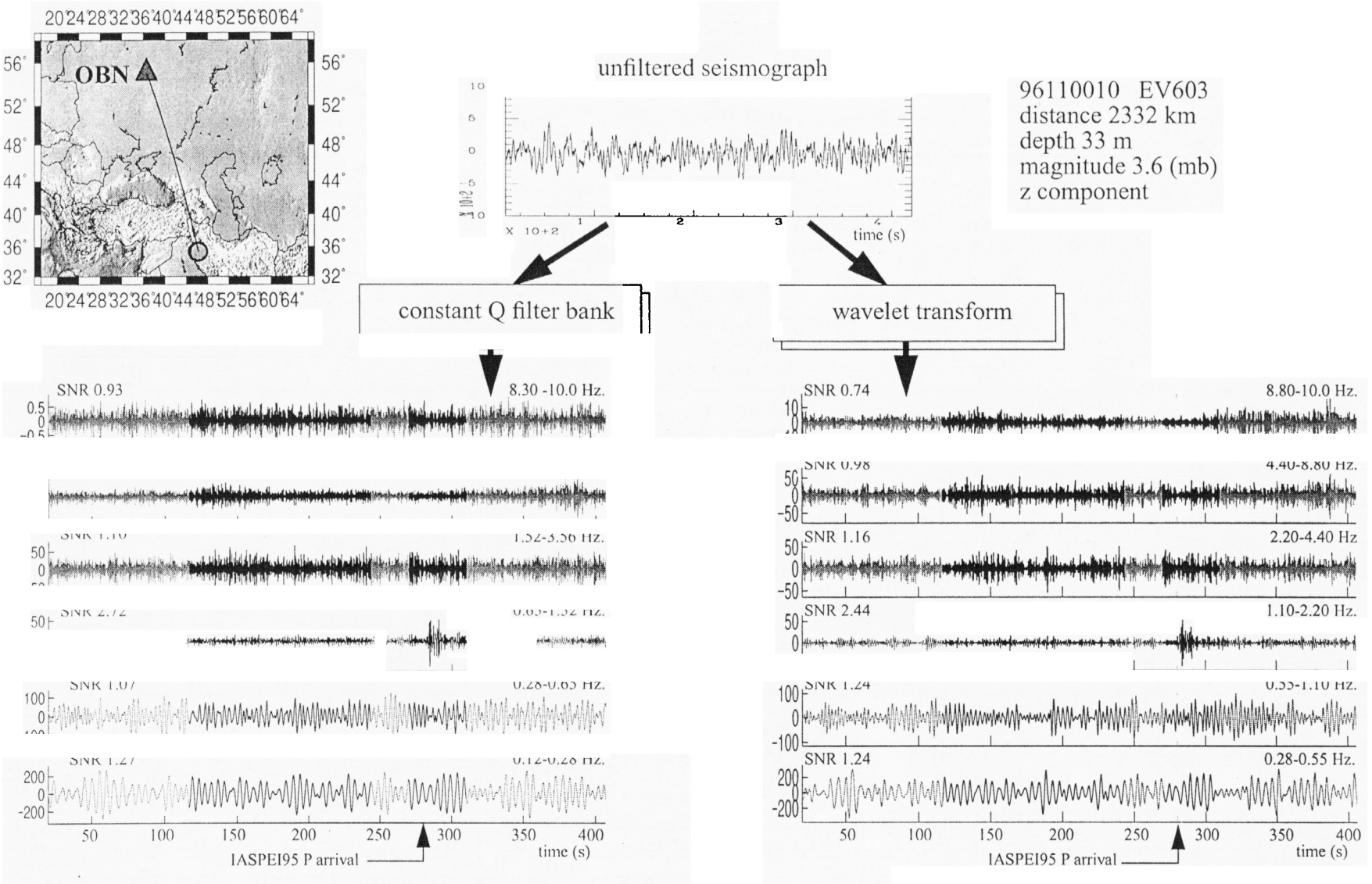

Figure 2.1.1 Decomposition of raw signal using wavelet transform (right) and constant Q logarithmic filter bank (left). In both cases, the fourth scale contains the dominant arrival energy. The wavelet scale corresponds to a 0.55-1.1 Hz filter, while the band in the filter bank is a 4th order Butterworth filter from 0.65-1.52 Hz.

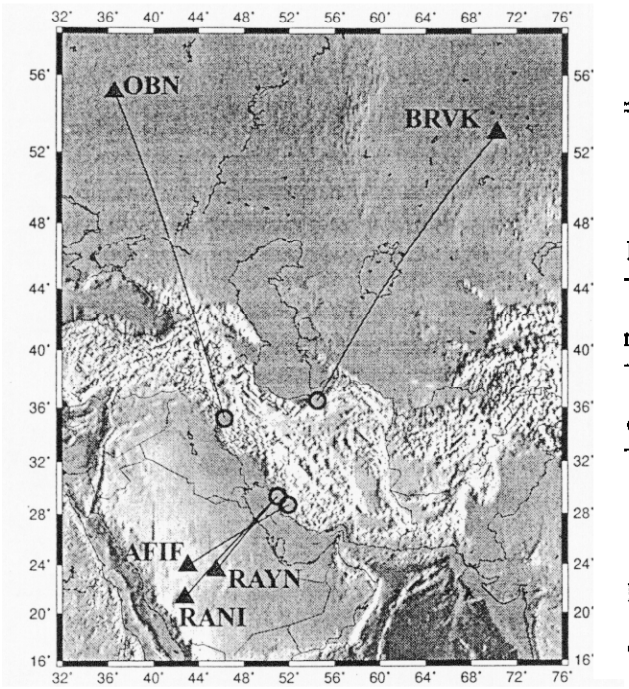

Station name	AFIF	RAYN	OBN	RANI	BRVK
station lat. (deg)	23.9	23.5	55.1	21.3	55.1
station lon. (deg)	43.0	45.5	36.6	42.8	36.6
event mag. (mb)	4.0	4.6	3.6	4.5	4.2
event depth (m)	33.0	79.0	33.0	33.0	0.0
event lat. (deg)	28.7	29.4	35.3	29.4	36.5
event lon. (deg)	51.9	51.0	46.3	51.0	54.5
dist. (km)	1041	848	2332	1216	2217

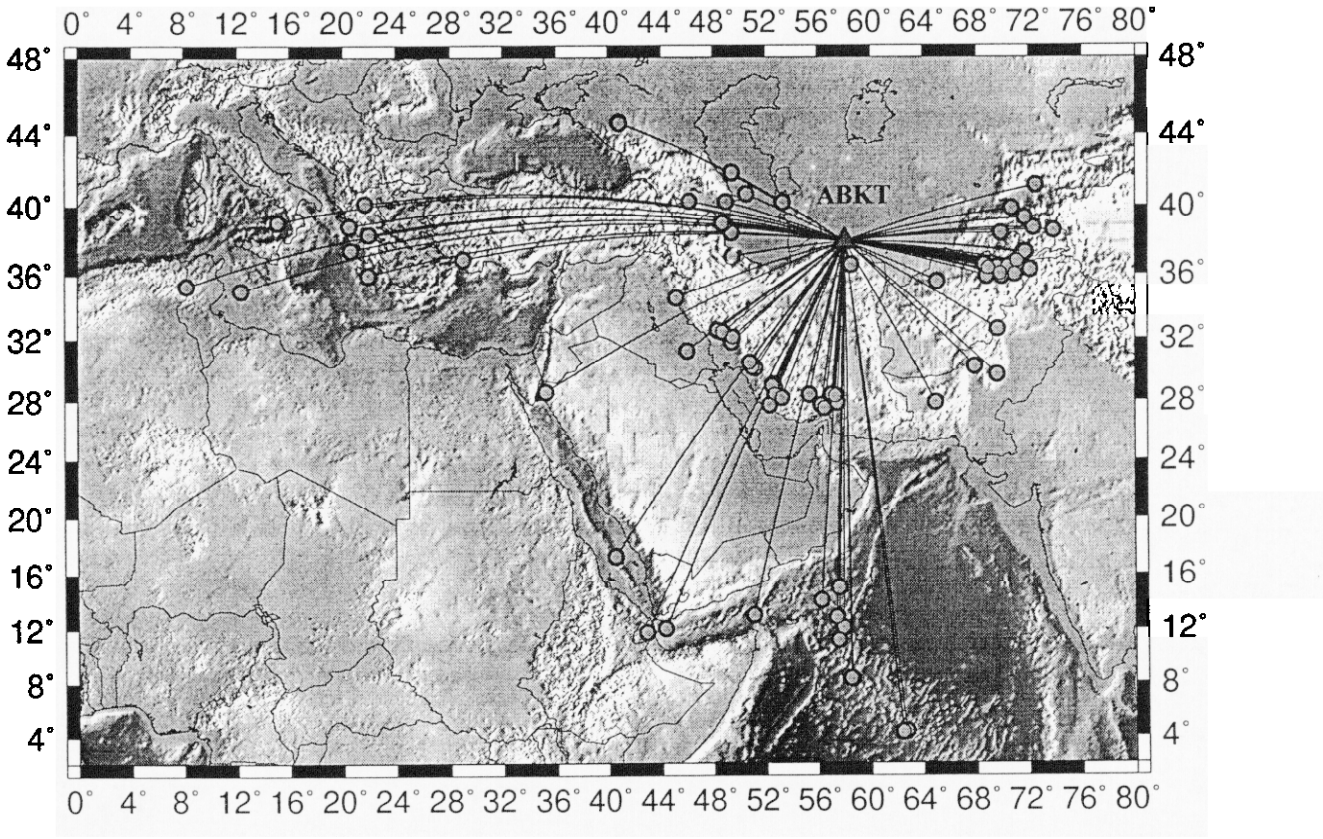

Figure 2.1.2 Map of low SNR regional event/station pairs selected by analyst based on difficulty on selecting a filter for picking the P arrival. for low SNR events.(top left) Corresponding table of values for event and station location, magnitude, distance, and depth. (top right) Location of 92 ABKT events to be filtered by the filter optimization algorithm to show regional propagation characteristics based on filter clusters. (bottom)

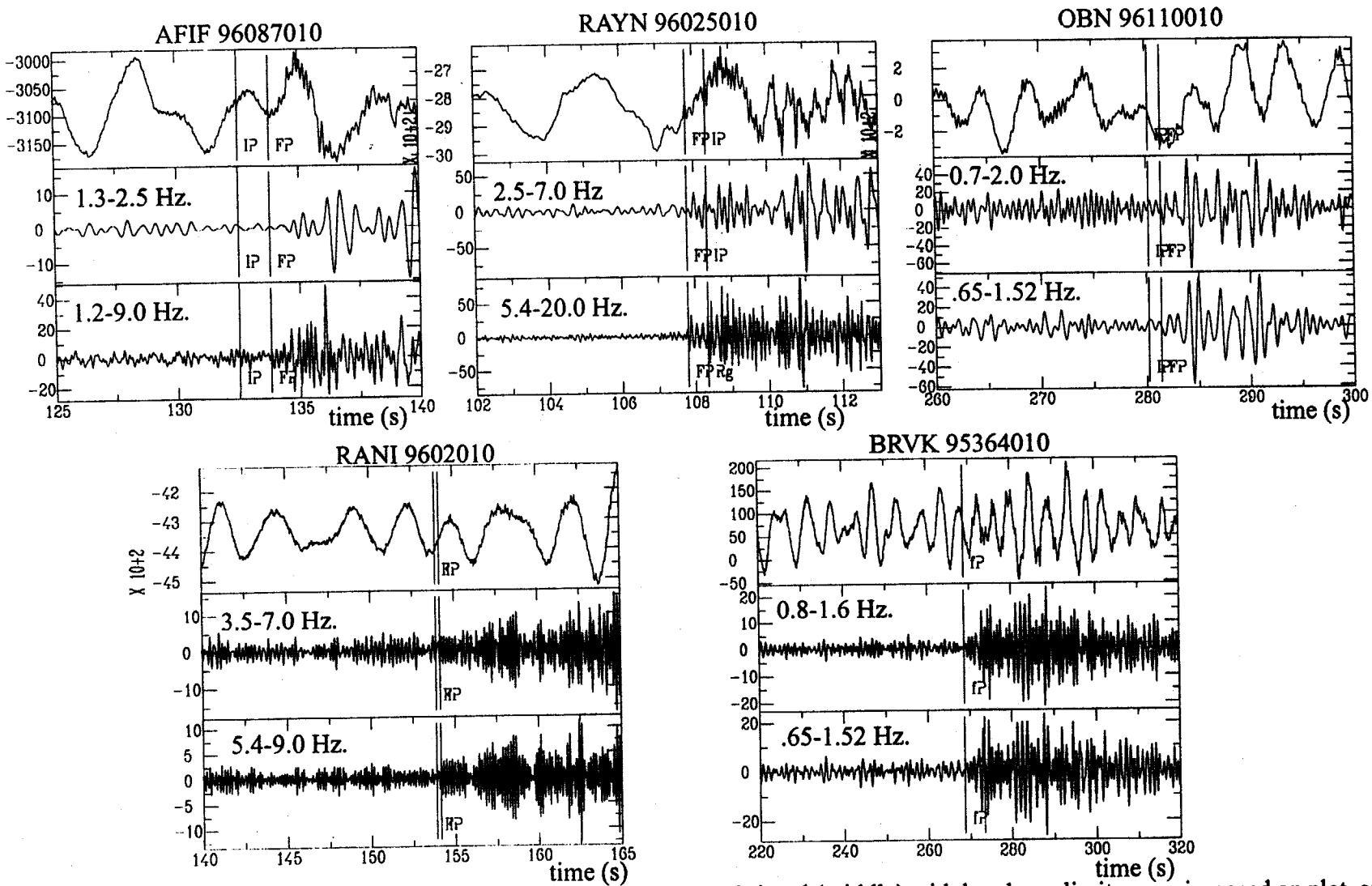

Figure 2.4.1 Five low SNR events with raw signal (top), analyst filtered signal (middle) with bandpass limits superimposed on plot, and optimization algorithm suggested filter (bottom) with bandpass limits superimposed on plot. IASPEI95 P arrival is indicated by the IP marker on each plot. Analyst pick is indicated by the FP marker. (The middle plots were used for the FP pick)

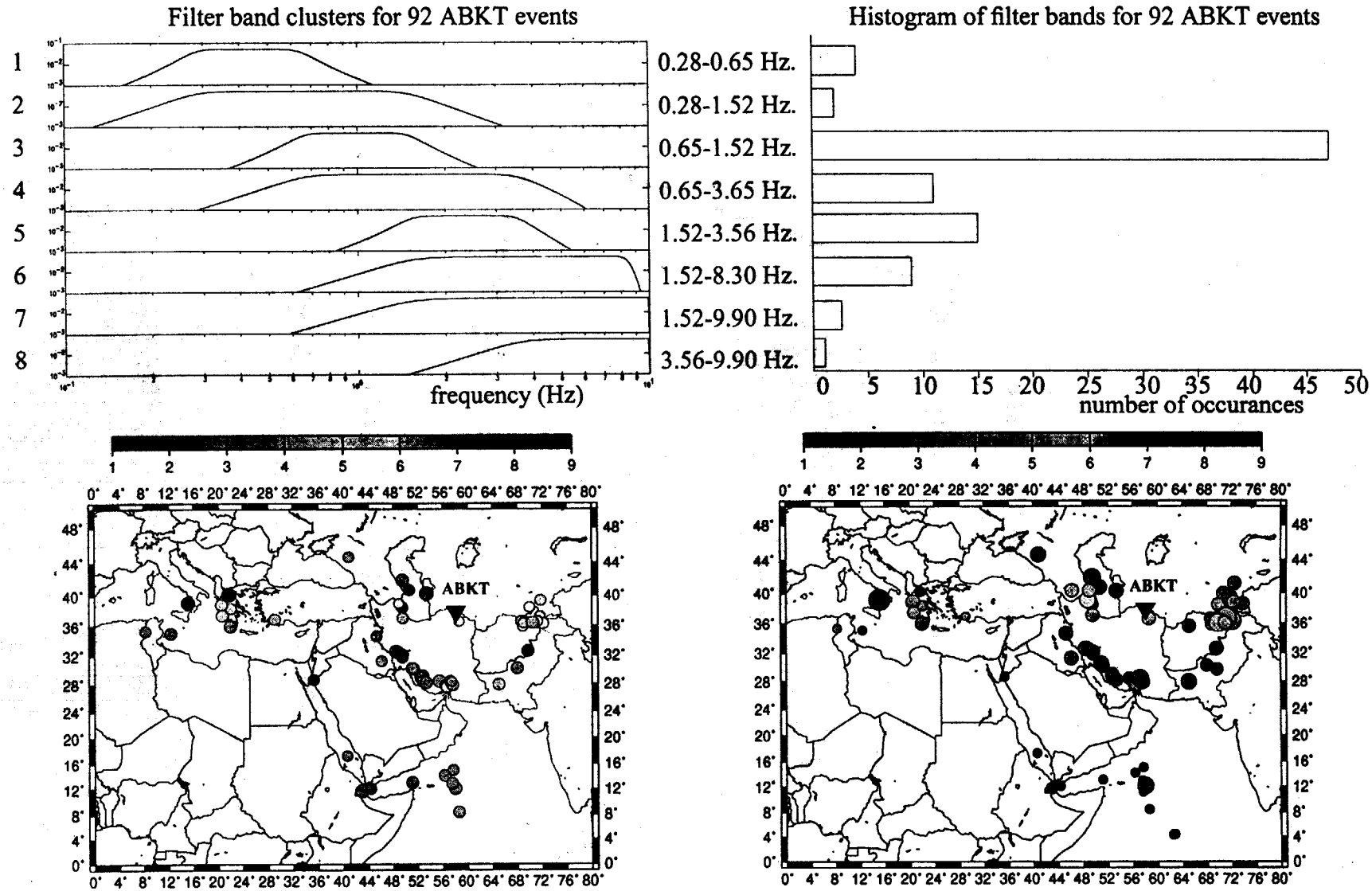

Figure 2.5.1 Clustering of 92 ABKT event bandpass filters revealed 8 unique clusters. (top left) Histogram indicates predominance for 3rd filter cluster, but also shows a wide variance for the region around ABKT. (top right) Maps indicate location of clusters sized by magnitude (bottom left) and sized by depth (bottom right)

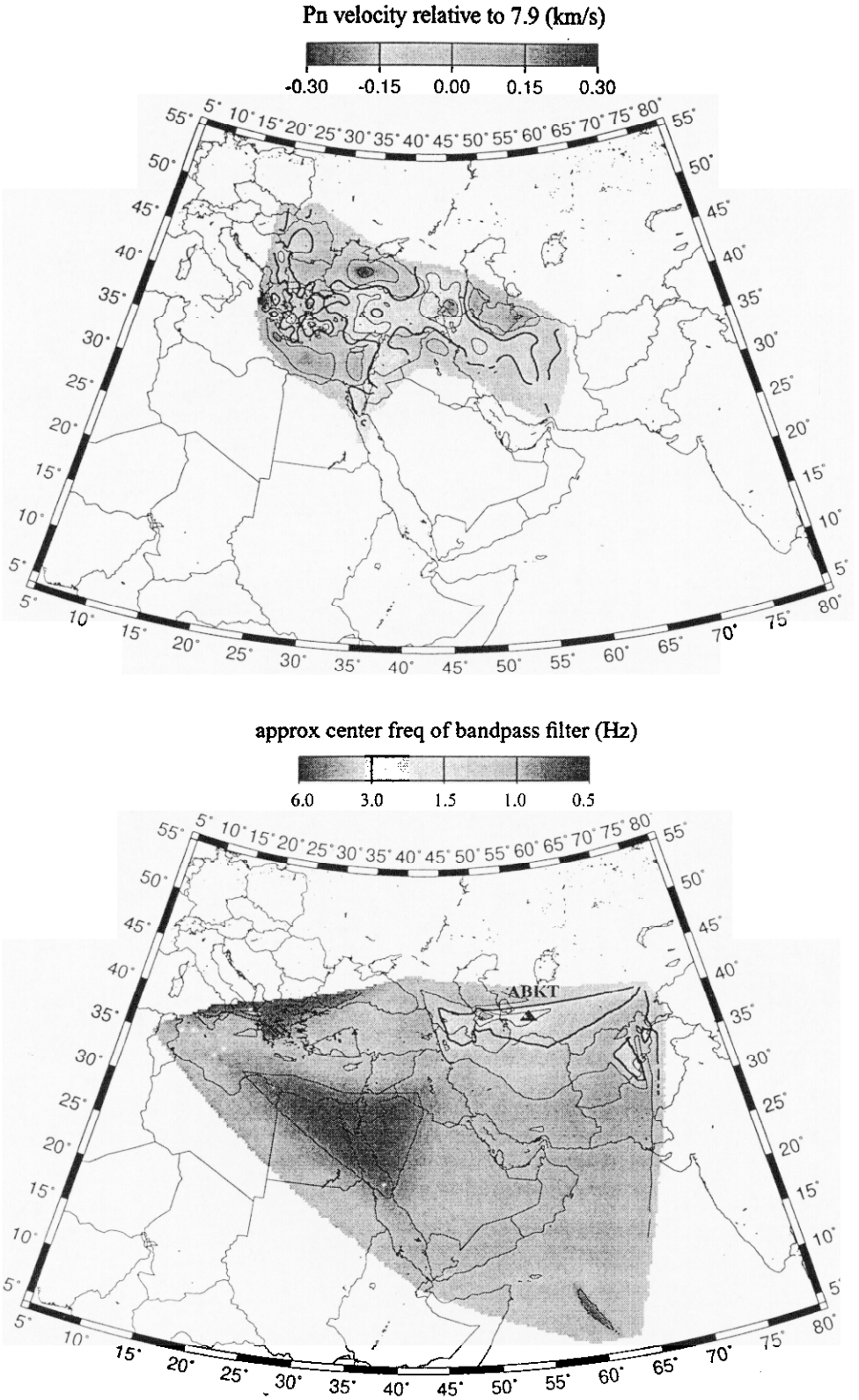

Figure 2.6.1 Plot of Pn velocity relative to 7.9 km/s (top). Contour plot of the approximate band-pass filter center frequencies for the 8 filter clusters produced by 92 ABKT events. (bottom)

Technical Information Department • **Lawrence Livermore National Laboratory**
University of California • Livermore, California 94551